



CFP/Yit: An Inbred Mouse Strain with Slow Gastrointestinal Transit

Gaku Wagai¹ · Masao Togao¹ · Takashi Kurakawa¹ · Haruka Nishizaki¹ · Jun Otsuka¹ · Yuki Ohta-Takada¹ · Akinobu Kurita¹ · Tomo Suzuki¹ · Koji Kawakami¹

Received: 19 September 2023 / Accepted: 26 March 2024
© The Author(s) 2024

Abstract

Background Gastrointestinal transit (GIT) is influenced by factors including diet, medications, genetics, and gut microbiota, with slow GIT potentially indicating a functional disorder linked to conditions, such as constipation. Although GIT studies have utilized various animal models, few effectively model spontaneous slow GIT.

Aims We aimed to characterize the GIT phenotype of CFP/Yit (CFP), an inbred mouse strain with suggested slow GIT.

Methods Female and male CFP mice were compared to Crl:CD1 (ICR) mice in GIT and assessed based on oral gavage of fluorescent-labeled 70-kDa dextran, feed intake, fecal amount, and fecal water content. Histopathological analysis of the colon and analysis of gut microbiota were conducted.

Results CFP mice exhibited a shorter small intestine and a 1.4-fold longer colon compared to ICR mice. The median whole-GIT time was 6.0-fold longer in CFP mice than in ICR mice. CFP mice demonstrated slower gastric and cecal transits than ICR mice, with a median colonic transit time of 4.1 h (2.9-fold longer). CFP mice exhibited lower daily feed intakes and fecal amounts. Fecal water content was lower in CFP mice, apparently attributed to the longer colon. Histopathological analysis showed no changes in CFP mice, including tumors or inflammation. Moreover, CFP mice had a higher Firmicutes/Bacteroidota ratio and a relative abundance of Erysipelotrichaceae in cecal and fecal contents.

Conclusions This study indicates that CFP mice exhibit slow transit in the stomach, cecum, and colon. As a novel mouse model, CFP mice can contribute to the study of gastrointestinal physiology and disease.

Keywords Gastrointestinal transit time · Fecal water content · Cecal microbiota · Fecal microbiota · Feed intake

Introduction

Gastrointestinal (GI) transit time (GITT) is defined as the interval between food ingestion and its evacuation. Recently, research has focused on the association of GITT with health and disease, including typical GI diseases as well as certain metabolic and neurological conditions [1]. GITT is influenced by various host and environmental factors, including sex, aging, genetics, medication use, diet, and gut microbiota [1, 2]. In particular, the digestion and absorption of nutrients, along with alterations in the gut microbiota, are closely linked to GITT [3].

It has been common practice to use animal models to investigate the influence of GI transit (GIT) on host health.

For example, drug-induced constipated mice and rats have been used in preclinical studies of laxatives [4]. These models have also revealed the interactions among diet, GITT, and gut microbiota [3] and the potential impact of gut microbiota associated with delayed GITT on host disease [5]. Additionally, delayed GITT can be induced by dietary changes [6, 7], microbiota transplantation [8], and oral administration of ice-cold saline [9]; it is also observed in mouse models of neurological disorders, such as in Parkinson's disease [10]. Animal models of spontaneous slow GIT, including genetically modified animals [11–13] and spontaneously mutated ones [14, 15], have also been used. Despite the availability of several animal models, the association of GITT with health and disease remains unclear. One reason is that these relationships are multifactorial and complex, and current models alone cannot adequately simulate them. Therefore, additional animal models that mimic various aspects observed in humans are expected [4]. In particular, a model of spontaneously delayed GITT, without genetic manipulation, may

✉ Gaku Wagai
gaku-wagai@yakult.co.jp

¹ Yakult Central Institute, 5-11 Izumi, Kunitachi-Shi, Tokyo 186-8650, Japan

have the advantage of providing new perspectives on these complex relationships.

CFP/Yit (CFP) is an inbred mouse strain derived from CF-1 mice. Although it has been suggested that CFP mice exhibit delayed transit time throughout the GI tract [16], certain characteristics, such as transit through specific segments of the GI tract and the phenotypes associated with delayed GITT, have not been thoroughly investigated.

This study aimed to characterize the GIT and related phenotypes of CFP mice compared to Crl:CD1 (ICR) mice and evaluate their potential as a model for slow GIT. In addition to the total GIT, anatomically segmented GITs were analyzed to clarify transit in the large intestine, which accounts for most of the total GITT [17]. Fecal water content, which is associated with colonic transit time [18], was also examined. Furthermore, the gut microbiota was analyzed to explore its potential involvement in the characteristics of the GIT in CFP mice.

Materials and Methods

Animals

CFP mice were bred in house, and ICR mice were obtained from The Jackson Laboratory Japan, Inc. (Kanagawa, Japan). Because the assignment to experimental groups was determined based on mouse strain and sex, no grouping was conducted, and no mice were excluded before the experiments.

All mice were housed in flat-bottomed cages with bedding (Pulsoft; Oriental Yeast Co., Ltd., Tokyo, Japan) and nesting material (Rodent Nesting Sheets™ and Bio-Huts™; Bio-Serv, Flemington, NJ, USA) under specific pathogen-free conditions. The animal housing was maintained at a relative humidity of 30%–70%, temperature of 20 °C–26 °C, and a 12-h light/dark cycle with lights turned on at 8:00 am. The mice were provided free access to pelleted feed (F-2; Funabashi Farm Co., Ltd., Chiba, Japan) and water. No mice were fasted before the experiments. At the end of the experiments, all mice were euthanized under 3.5% isoflurane (isoflurane inhalation anesthetic solution; Pfizer Japan Inc., Tokyo, Japan) to collect GI tissues and contents and other materials for subsequent analyses as described below.

Study Design

As shown in Fig. 1, this study comprised five experiments involving a total of 24 female and 30 male CFP mice and an equal number of ICR mice. Each experiment included four groups based on strain and sex, with six mice per group; however, Experiment 4 involved six male CFP mice and six male ICR mice. In Experiment 1, whole GITT (WGTT) and mean retention time (MRT) as indices of total GI tract

transit. In the same mice, gastric emptying rate and small intestinal (SI) geometric center were measured. Anatomically segmented GIT was also evaluated in Experiment 2 by gastric and cecal retention times and SI and colonic transit times. In Experiment 3, amounts of cecal and colonic contents and their respective water contents were measured, which could be affected by large intestinal transit. The fecal water content was measured using feces collected within 1 h of GITT and MRT measurements in Experiment 1 and at age 11–12 weeks in Experiment 3 and collectively analyzed. In Experiment 4, histopathological analysis of the colon was conducted and thickness of the colonic muscle layer was determined. In Experiment 5, cecal and fecal microbiota, which exhibit a bidirectional relationship with large intestinal transit, were analyzed. Body weight and intestinal length were measured in Experiments 1–3 and analyzed collectively.

Body Weight and Intestinal Length

The body weight and intestinal length of 11–12-week-old mice were measured. SI length was defined as the distance from the pylorus to the ileocecum, and the colonic length was defined as the distance from the cecocolic junction to the anus.

Whole-GIT

Mice were housed in same-strain and -sex pairs for 3 weeks before the experiment. To evaluate WGTT and MRT in mice housed in pairs instead of individually, two types of transit markers were used. Specifically, 5 mg/mL of 70-kDa dextran, labeled with tetramethylrhodamine isothiocyanate (TRITC-dextran; TdB Labs, Uppsala, Sweden), and fluorescein isothiocyanate (FITC-dextran; TdB Labs) were prepared in phosphate-buffered saline (PBS). At the age of 10–11 weeks, 0.1 mL of TRITC-dextran solution was orally administered to one mouse per cage, and 0.1 mL of FITC-dextran solution was administered to the other mouse between 8:15 and 8:50 am. Feces were collected at 0.5, 1, 2, 3, 4, 5, 6, 7, 8, 9, 10, 11, 24, 26, 28, 30, 32, 34, and 48 h after marker administration. The fecal samples were freeze-dried, homogenized using 30 volumes of PBS (v/w), and left overnight at 4 °C. The fecal homogenates were centrifuged at 300×g for 3 min, and the supernatant was collected. Fluorescence intensity of the supernatant was measured in a microplate reader (Infinite® 200 PRO; Tecan Group Ltd., Männedorf, Switzerland) at 580-nm excitation and 547-nm emission for TRITC and at 522-nm excitation and 495-nm emission for FITC. The concentrations of TRITC-dextran and FITC-dextran were interpolated using a standard curve.

WGTT was defined as the time from the oral administration of the marker solution to the time of the first excretion of

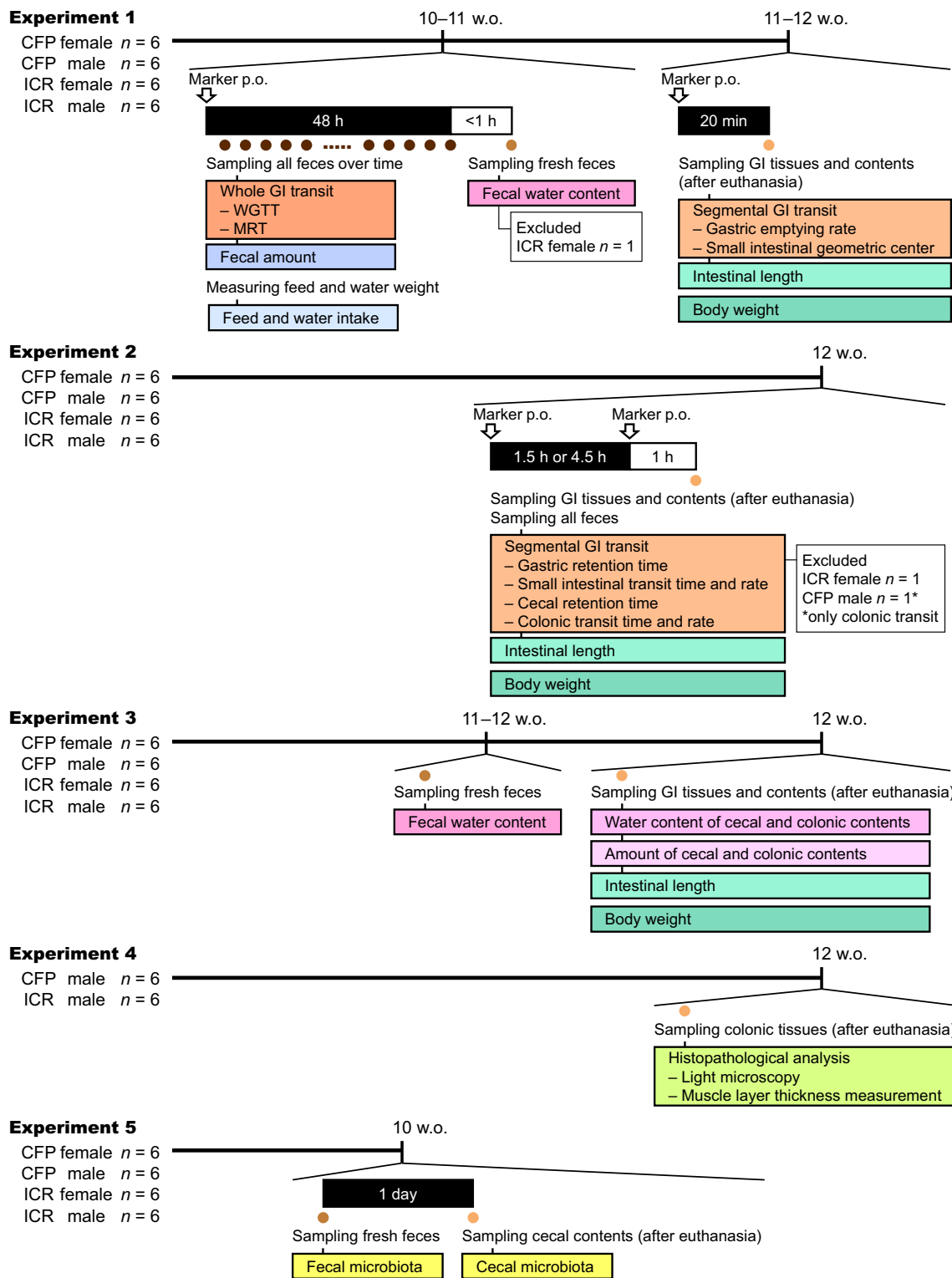


Fig. 1 Study design. In Experiment 1, WGTT and MRT were measured as indices of total GI tract transit. In the same mice, gastric emptying rate and small intestinal geometric center were measured. In Experiment 2, anatomically segmented GI transit was evaluated using a mathematical model. In Experiment 3, cecal and colonic contents as well as their water contents were measured. In Experiment 4, his-

topathological analysis of the colon was conducted and thickness of the colonic muscle layer was determined. In Experiment 5, cecal and fecal microbiota were analyzed. Body weight, intestinal length, and fecal water content were measured in several experiments and analyzed collectively. *GI* gastrointestinal, *WGTT* whole GI transit time, *MRT* mean retention time, *w.o.* weeks old, *p.o.* peroral administration

feces in which the marker was detected [19]. In cases where no marker was detected in the feces until 11 h after marker administration, the WGTT was recorded as 11 h. MRT was calculated using the formula $\Sigma (x_i \cdot t_i) / \Sigma x_i$, where t_i denotes the time to fecal excretion following marker administration and x_i denotes the amount of the marker collected at time t_i [20, 21]. The time of fecal excretion was defined as the interval between the fecal collection time and the previous collection time.

GI Segment-Specific Transit

Gastric Emptying Rate and SI Geometric Center

Gastric and SI transits were evaluated 2–6 days after measuring MRT. Mice were orally administered 0.5 mg/0.1 mL/mouse of 70-kDa FITC-dextran between 8:05 and 10:35 am. After 20 min, the mice were euthanized by cervical dislocation following cardiac blood sampling under anesthesia as described above. Immediately, the stomach, small intestine, cecum, and colon were collected. The small intestine was divided into 10 equal parts. Each GI segment and its contents were placed in 1 mL of PBS for each SI segment and 10 mL for others. The GI content samples were centrifuged as described above, and the supernatants were collected. The concentrations of FITC-dextran in the supernatant and diluted plasma were determined following the procedure described above.

Gastric emptying was calculated as the proportion of the amount of marker collected from the contents of the intestinal tract to the total amount of marker collected [22]. The SI geometric center, an index of SI transit, was calculated using the formula $\Sigma (x_j \cdot j) / \Sigma x_j$, where j denotes the segment number (0, stomach; 1–10, small intestine; 11, cecum; 12, colon), and x_j denotes the amount of marker collected in segment j [22].

Gastric and Cecal Retention Times and SI and Colonic Transit Times

Mice were housed in same-strain and -sex pairs for at least 2 weeks before the experiment. At the age of 12 weeks, the mice were orally administered 0.5 mg/0.1 mL/mouse of 70-kDa TRITC-dextran and 70-kDa FITC-dextran. In each cage, one mouse received the TRITC-dextran dose first, followed by the FITC-dextran dose, and the other mouse received these doses in the reverse order. The dosing interval between the two markers was 4.5 h for CFP mice and 1.5 h for ICR mice to account for the difference in GITT between these strains, with the first dosing occurring between 8:05 and 9:45 am. After 1 h of the second dose, the mice were euthanized as described above. Immediately, the stomach, small intestine, cecum, and colon were collected. The colon was divided into four equal parts. Each GI segment and its contents were placed in 2 mL of PBS for the stomach and cecum, 5 mL for the small intestine, and 1 mL for each colonic segment. The sampled GI contents were

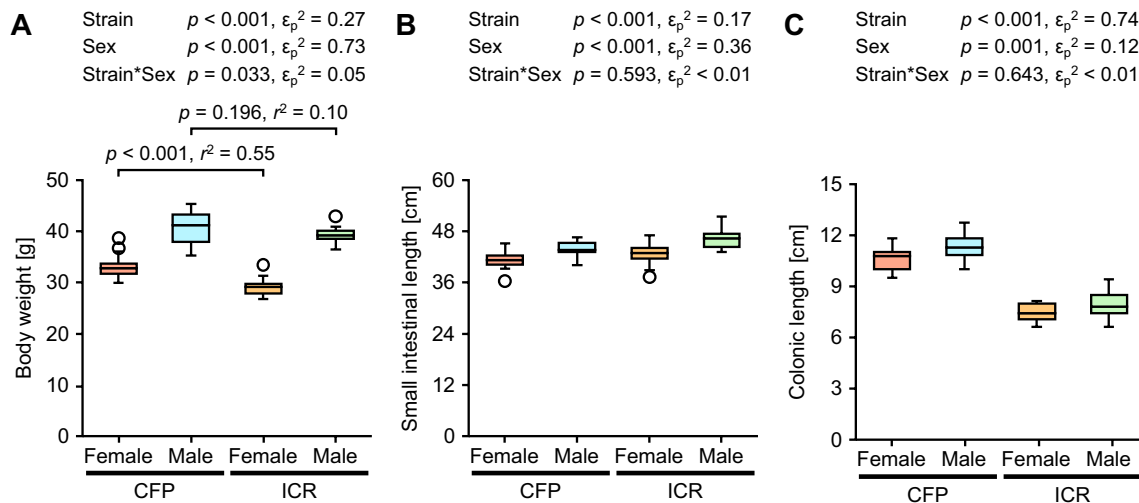
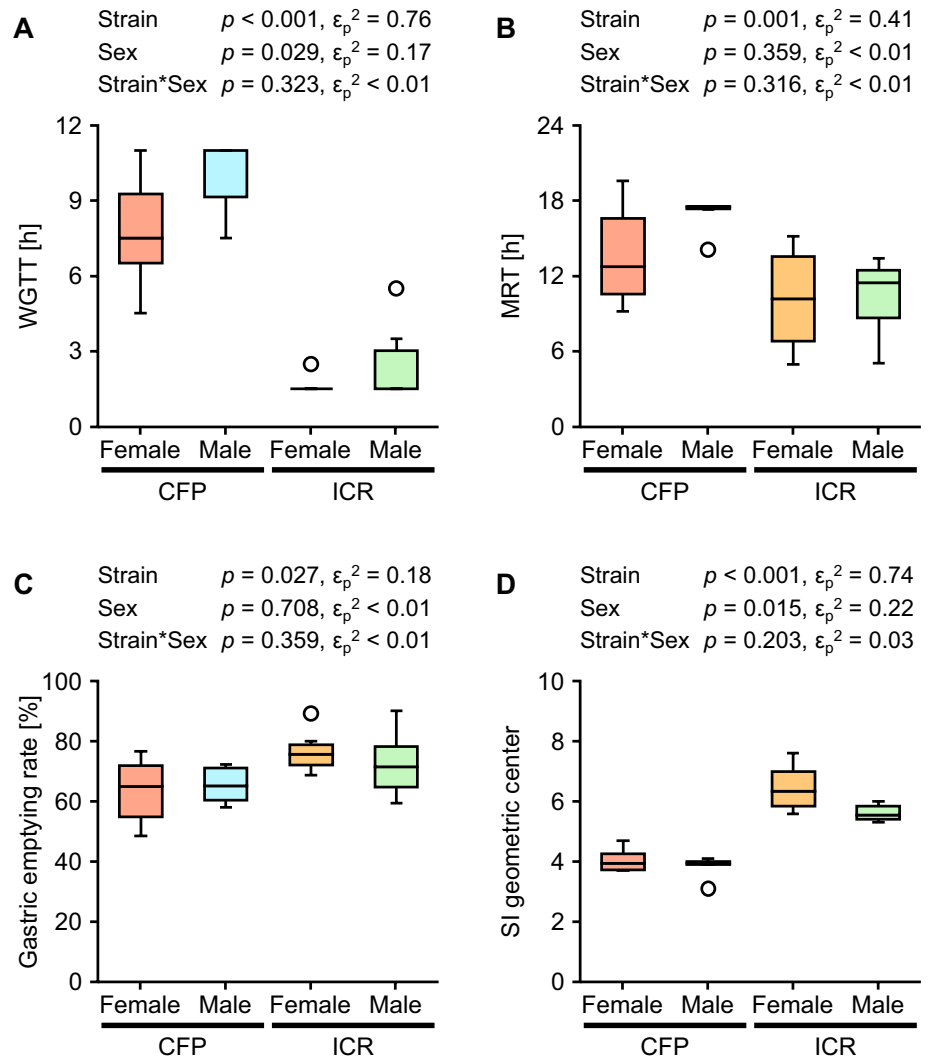


Fig. 2 Comparison of body weight and intestinal length between CFP and ICR mice. Body weight (**A**) and length of the small intestine (**B**) and colon (**C**) were measured at the age of 11–12 weeks ($n = 18$ per group). The box plot shows the median and IQR with whiskers extending to the minimum and maximum values within 1.5 times of the IQR from the hinge of the box; data points outside 1.5 times the IQR are shown as circles. Effects of mouse strain (CFP vs. ICR) and

sex (female vs. male) and their interaction (Strain*Sex) were analyzed using ART two-way ANOVA; p values and effect sizes (ϵ_p^2) are shown at the top. In case of significant interactions, p values and effect sizes (r^2) of the post hoc Steel–Dwass test are shown immediately above the plot. See Online Resource 3 for results of other post hoc analyses. IQR interquartile range, ART aligned rank transform, ANOVA analysis of variance

Fig. 3 Comparison of complete GI, gastric, and SI transit between CFP and ICR mice. The total GIT was evaluated in terms of WGTT (A) and MRT (B) at the age of 10–11 weeks ($n=6$ per group). Gastric and SI transits were evaluated in terms of the gastric emptying rate (C) and SI geometric center (D) at the age of 11–12 weeks ($n=6$ per group). The box plot shows the median and IQR with whiskers extending to the minimum and maximum values within 1.5 times of the IQR from the hinge of the box; data points outside 1.5 times the IQR are shown as circles. Effects of mouse strain (CFP vs. ICR) and sex (female vs. male) and their interaction (Strain*Sex) were analyzed using ART two-way ANOVA; p values and effect sizes (ϵ_p^2) are shown at the top. See Online Resource 3 for results of post hoc analyses. GI gastrointestinal, SI small intestinal, GIT GI transit, WGTT whole GIT time, MRT mean retention time, IQR interquartile range, ART aligned rank transform, ANOVA analysis of variance



centrifuged as described above, and the supernatants were collected. Additionally, all feces in the cages were collected, and marker extracts were obtained as described above. The concentrations of TRITC-dextran and FITC-dextran in the supernatants, fecal marker extracts, and diluted plasma were determined as described above. One female ICR mouse was excluded from the analysis owing to the suspicion of having ingested the excreted marker through feces, which was indicated by a higher proportion of the first dose marker than the second dose marker in the stomach.

Gastric, SI, cecal, and colonic transits were estimated using previously reported model equations [20]. Briefly, the stomach and cecum were treated as compartments and their contents were assumed to flow out with their own specific rate constants. The reciprocals of these rate constants were considered as the retention times of the stomach and cecum. The SI transit time was defined as the time taken for the marker excreted from the stomach to reach the cecum. In the colon, transit times were calculated for each of the four

equal segments. The transit time of a segment was defined as the interval between marker excretion from the cecum or a previous segment and excretion into the next segment or feces. The colonic transit time was, therefore, the sum of the transit times of these four segments. These retention and transit times were estimated for each mouse using the nonlinear least squares method with the Excel Solver add-in (Microsoft® Excel® 2013; Microsoft Corporation, Seattle, WA, USA). Initial values were determined using the grid search method. However, for one male CFP mouse in which the most distal arrival site of the first dose marker was the third quarter colonic segment, the transit time of the third- and fourth-quarter colons and the entire colon could not be calculated.

Feed and Water Intake and Fecal Excretion

Feed and water intake were measured for each cage during the 48-h period of WGTT and MRT measurements,

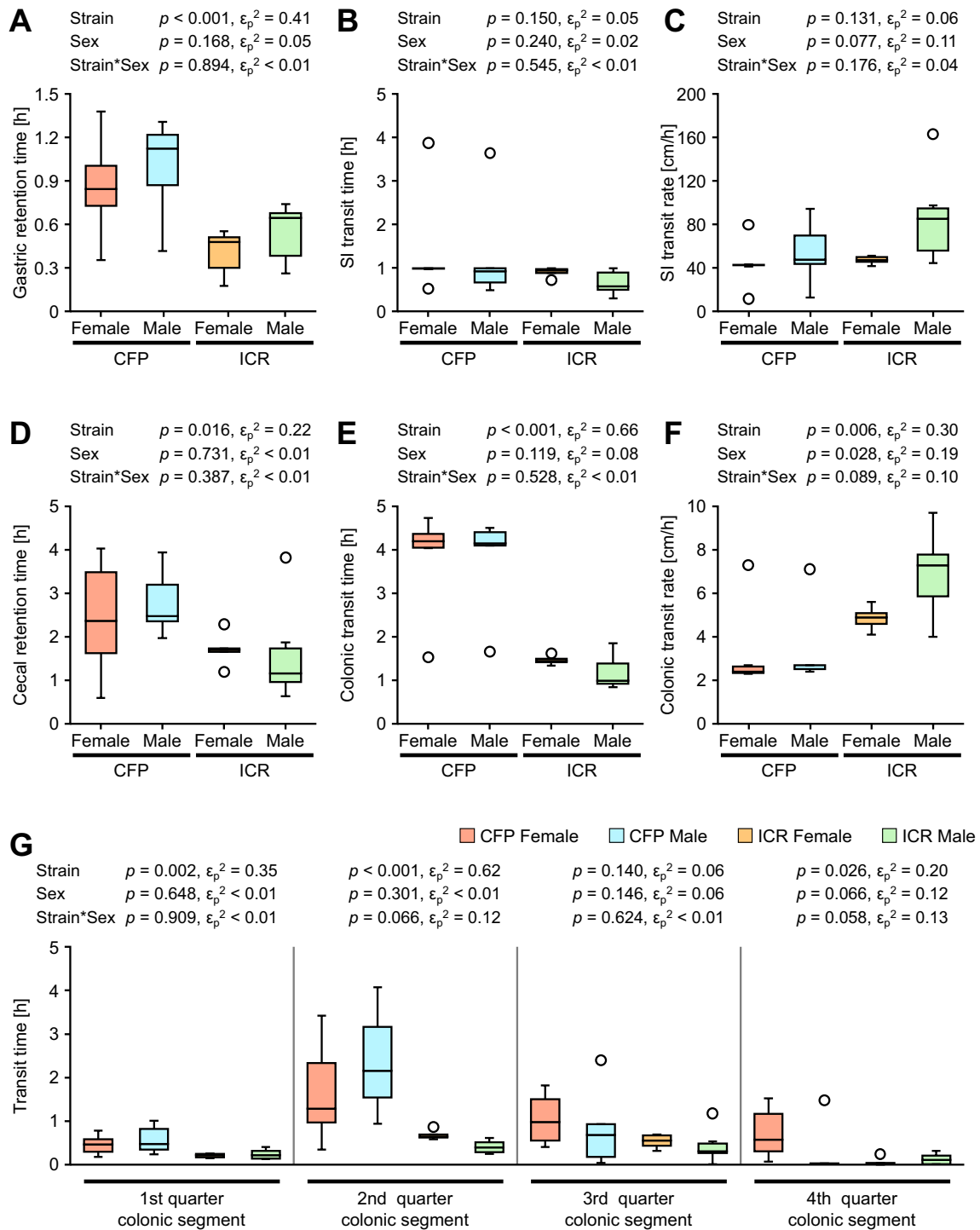


Fig. 4 Comparison of the transit of anatomically segmented gastrointestinal tract between CFP and ICR mice. At the age of 12 weeks, gastric retention time (A), SI transit time (B) and rate (C), cecal retention time (D), and colonic transit time (E) and rate (F) were estimated using a mathematical model. Additionally, four divided colonic transit times (G) were estimated. $n=6$ per group, except for female ICR mice ($n=5$) and colonic transit time and rate and for third- and fourth-quarter colonic segments in male CFP mice ($n=5$). The box plot shows the median and IQR with whiskers extending to the mini-

um and maximum values within 1.5 times of the IQR from the hinge of the box; data points outside 1.5 times the IQR are shown as circles. Effects of mouse strain (CFP vs. ICR) and sex (female vs. male) and their interaction (Strain*Sex) were analyzed using ART two-way ANOVA; p values and effect sizes (ϵ_p^2) are shown at the top. See Online Resource 3 for results of post hoc analyses. *SI* small intestinal, *IQR* interquartile range, *ART* aligned rank transform, *ANOVA* analysis of variance

and the daily amounts of feed and water intake per mouse were determined. The dry weight of feces and the number of fecal pellets excreted per mouse per day were calculated for each cage using the feces collected during WGTT and MRT measurements.

Fecal Water Content

At the age of 10–12 weeks, fresh feces were collected between 8:15 and 9:10 am. Fecal water contents were calculated using the formula $((w_{ff} - w_{df})/w_{ff}) \times 100$, where w_{ff} and w_{df} denote the weight of the fresh and freeze-dried feces, respectively.

Amount and Water Content of Cecal and Colonic Contents

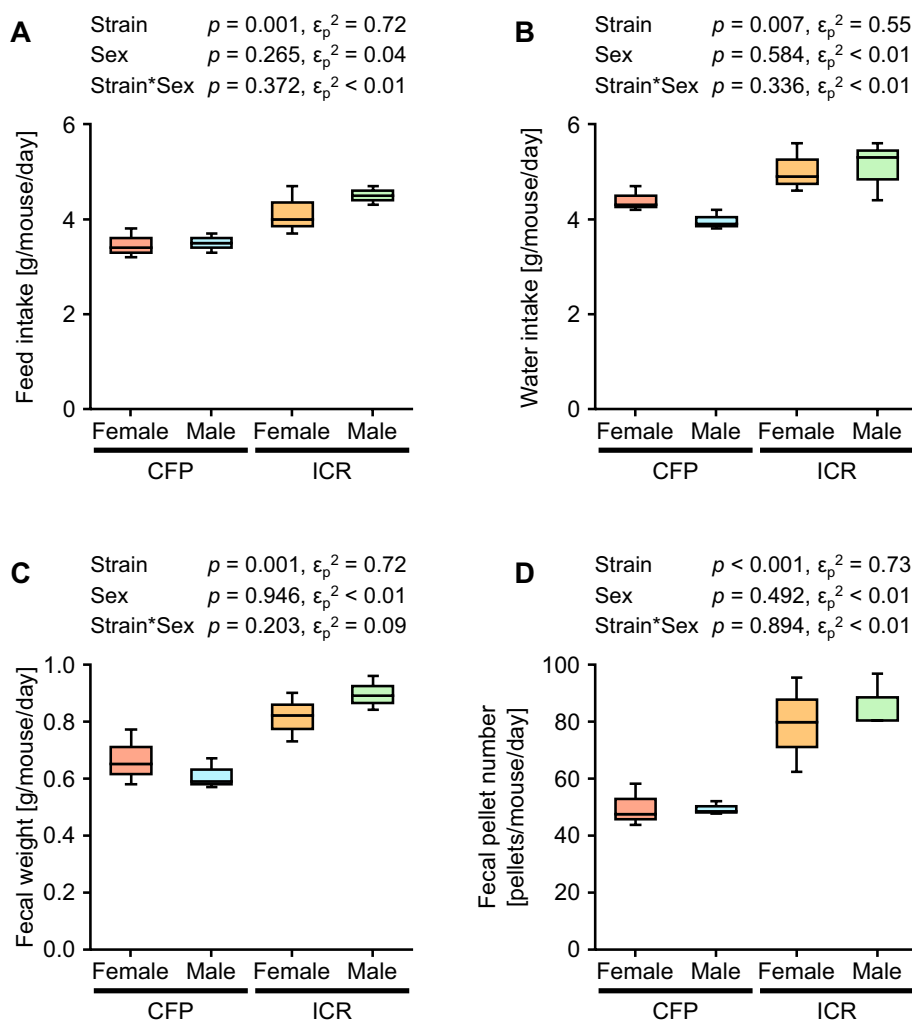
Mice were housed in same-strain and -sex pairs for 4 weeks before the experiment. At the age of 12 weeks, the mice

were euthanized between 8:00 and 10:30 am as described above, without blood collection. After rapidly measuring the distance of the colonic content from the cecocolic junction, cecal and colonic contents were collected. Colonic contents were collected every 2 cm from the cecocolic junction. The cecal and colonic water contents were calculated using the same method as the fecal water content described above.

Histopathological Analysis

Male mice were housed in same-strain pairs for at least 3 weeks before the experiment. At the age of 12 weeks, the mice were euthanized by exsanguination under anesthesia, as described above, between 9:00 and 11:30 am. The colon was collected and divided at half the length from the cecocolic junction to the anus. The proximal and distal sides from the center of the colon were then divided into 2-cm units. Each sample was fixed in 10% neutral-buffered formalin (Mildform® 10N; FUJIFILM Wako Pure Chemical

Fig. 5 Comparison of feed and water intake and fecal excretion between CFP and ICR mice. Feed intake (A), water intake (B), dried fecal weight (C), and fecal pellet number (D) were measured at the age of 10–11 weeks ($n = 3$ per group). The box plot shows the median and IQR with whiskers extending to the minimum and maximum values within 1.5 times of the IQR from the hinge of the box. Effects of mouse strain (CFP vs. ICR) and sex (female vs. male) and their interaction (Strain*Sex) were analyzed using ART two-way ANOVA; p values and effect sizes (ϵ_p^2) are shown at the top. See Online Resource 3 for results of post hoc analyses. *IQR* interquartile range, *ART* aligned rank transform, *ANOVA* analysis of variance



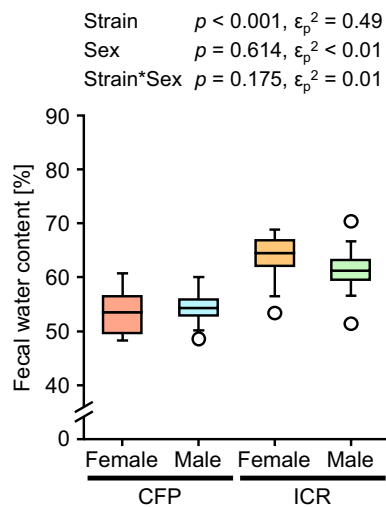


Fig. 6 Comparison of fecal water content between CFP and ICR mice. Fecal water content was measured at the age of 10–12 weeks. $n = 12$ per group, except for female ICR mice ($n = 11$). The box plot shows the median and IQR with whiskers extending to the minimum and maximum values within 1.5 times of the IQR from the hinge of the box; data points outside 1.5 times the IQR are shown as circles. The effects of mouse strain (CFP vs. ICR) and sex (female vs. male) and their interaction (Strain*Sex) were analyzed using ART two-way ANOVA; p values and effect sizes (ϵ_p^2) are shown at the top. See Online Resource 3 for results of post hoc analyses. *IQR* interquartile range, *ART* aligned rank transform, *ANOVA* analysis of variance

Corporation, Osaka, Japan) for approximately 24 h and embedded in paraffin wax. The paraffin-embedded samples were sectioned longitudinally at about 4- μ m thickness and stained with hematoxylin–eosin. Each section was examined under a light microscope by one pathologist in a blinded manner. Additionally, the thickness of the colonic muscle layer was measured at the first unit distal to the center of the colon using ImageJ (version 1.53c, Java 1.8.0_172) [23] at six points in the area that contained contents, and the average value was determined. Samples without contents were excluded from the evaluation.

Cecal and Fecal Microbiota Analysis

Collection of Feces and Cecal Contents

Mice were housed in same-strain and -sex groups of six per cage for 3 weeks before the collection of feces and cecal contents. At the age of 10 weeks, fresh feces were collected between 1:00 and 3:20 pm and stored at -80°C until use. The day after fecal collection, mice were euthanized by exsanguination under anesthesia, as described above, between 9:00 am and 12:00 pm. Cecal contents were immediately collected and stored at -80°C until use.

Bacterial DNA Extraction

For bacterial DNA extraction, cecal contents and fecal samples were homogenized with nine volumes of PBS (v/w). For 200 μL of homogenate, 250 μL of Tris–EDTA (TE) buffer solution, 50 μL of 10% sodium dodecyl sulfate solution, 0.3 g of glass beads (0.1 mm diameter), and 500 μL of TE-saturated phenol were added. The mixture was vigorously shaken for 15 min using ShakeMaster[®] (BioMedical Sciences, Tokyo, Japan). Following centrifugation at $20,630\times g$ for 5 min, 400 μL of supernatant was collected. An equal volume of phenol/chloroform/isoamyl alcohol (25:24:1) was added to the supernatant. The mixture was vigorously shaken for 15 s. After centrifugation at $20,630\times g$ for 5 min, 250 μL of supernatant was collected and purified via isopropanol precipitation. After rinsing with 80% ethanol, the DNA was suspended in 1 mL of TE buffer and stored at -30°C until use.

16S rRNA Gene Amplicon Sequencing

The V4 region of the bacterial 16S rRNA gene was amplified and sequenced according to a previously described method [24], with minor modifications [25]. Briefly, bar-coded amplicons were obtained through PCR using the primers 515F (5'-GTGCCAGCMGCCGCGGTAA-3') and 806R (5'-GGACTACHVGGGTWTCTAAT-3'), TB Green[®] Premix Ex Taq[™] II (Tli RNaseH Plus) (Takara Bio Inc., Shiga, Japan), and DNA extracted from each sample in an Applied Biosystems 7500 Real-Time PCR System (Applied Biosystems, Foster City, CA, USA). The thermal cycler program was set as follows: 95°C for 30 s, followed by 40 cycles at 95°C for 5 s, 50°C for 30 s, and 72°C for 40 s. The reaction was immediately stopped before the amplification reached a plateau. Subsequently, the amplicons obtained were purified and quantified using Agencourt AMPure XP (Beckman Coulter Inc., Brea, CA, USA) and QuantiFluor[®] dsDNA System (Promega, Madison, WI, USA). The purified amplicons were pooled in equimolar amounts and sequenced using the MiSeq Reagent Kit v2 (500 cycles) (Illumina, Inc., San Diego, CA, USA) on a MiSeq[®] System (Illumina, Inc.).

Meta 16S rRNA Gene Analysis

The raw sequence data were processed in QIIME2 [26] (version 2021.4) using the Silva database (version 138_1) as a reference to generate a feature table (Online Resource 1) and determine relative abundances at the bacterial phylum and family levels. Differences in microbiota between samples were assessed based on unweighted and weighted UniFrac distances and visualized using principal coordinate analysis (PCoA) conducted with QIIME2. Alpha diversity indices, including observed features, the

Shannon index, and Faith's phylogenetic diversity (Faith's PD), were calculated using QIIME2.

Statistical Analysis

The data are presented as medians and interquartile ranges. The effects of mouse strain, sex, and their interactions were analyzed using an aligned rank transform (ART) [27] two-way analysis of variance (ANOVA). Additionally, the effects of mouse strain, sampling source, and their interactions were analyzed using ART two-way repeated measures ANOVA. For post hoc analysis, the Steel–Dwass test or Mann–Whitney U test was used for unpaired data and Wilcoxon signed-rank test was used for paired data. The Mann–Whitney U test and Wilcoxon signed-rank test underwent Bonferroni correction. Differences in muscle layer thickness were analyzed using Welch's t test. Microbiota differences between CFP and ICR mice and between cecal and fecal contents were evaluated using permutational multivariate ANOVA (PERMANOVA). Statistical tests were performed using Bell Curve for Excel version 4.05 (Social Survey Research Information Co., Ltd., Tokyo, Japan), except for PERMANOVA, which was performed using QIIME2. A significance threshold of $p < 0.05$ was applied. Effect size was determined using partial epsilon squared (ϵ_p^2) and r -squared (r^2).

Results

Body Weight and Intestinal Length

The interaction between mouse strain and sex was significant for body weight ($p = 0.033$, $\epsilon_p^2 = 0.05$; Fig. 2A). In females, CFP mice weighed more than ICR mice ($p < 0.001$, $r^2 = 0.55$), but no significant difference was observed in males ($p = 0.196$, $r^2 = 0.10$). SI and colonic lengths were shorter in females than in males ($p < 0.001$, $\epsilon_p^2 = 0.36$ for SI length, $p = 0.001$, $\epsilon_p^2 = 0.12$ for colonic length; Fig. 2B and C). The SI length was shorter in CFP mice than in ICR mice ($p < 0.001$, $\epsilon_p^2 = 0.17$; Fig. 2B). In contrast, the colon was longer in CFP mice than in ICR mice, with a median length of 1.4-fold longer ($p < 0.001$, $\epsilon_p^2 = 0.74$; Fig. 2C).

Whole-GIT

Whole-GIT was evaluated based on WGTT and MRT. The median WGTT was 2.5-fold longer in CFP mice than in ICR mice ($p < 0.001$, $\epsilon_p^2 = 0.76$; Fig. 3A). Although the orally administered markers in all ICR mice appeared in excreted feces by 6 h after the administration of the marker, the

markers had not been excreted even 11 h after administration in one female and four male CFP mice.

The MRT was also longer in CFP mice than in ICR mice ($p = 0.001$, $\epsilon_p^2 = 0.41$; Fig. 3B), with no significant differences between females and males ($p = 0.359$, $\epsilon_p^2 < 0.01$). In both strains, > 98% of the collected markers were excreted within first 24 h.

GI Segment-Specific Transit

Gastric Emptying Rate and SI Geometric Center

To assess gastric and SI transits, the gastric emptying rate and SI geometric center were measured. No fluorescence from the administered marker was detected in the plasma of any of the mice, indicating minimal absorption of the orally administered marker. The gastric emptying rate was lower in CFP mice than in ICR mice ($p = 0.027$, $\epsilon_p^2 = 0.18$; Fig. 3C), with no significant difference observed between females and males ($p = 0.708$, $\epsilon_p^2 < 0.01$). The SI geometric center was also smaller in CFP mice than in ICR mice ($p < 0.001$, $\epsilon_p^2 = 0.74$; Fig. 3D) and was higher in females than in males ($p = 0.015$, $\epsilon_p^2 = 0.22$).

Gastric Retention Time and SI Transit Time

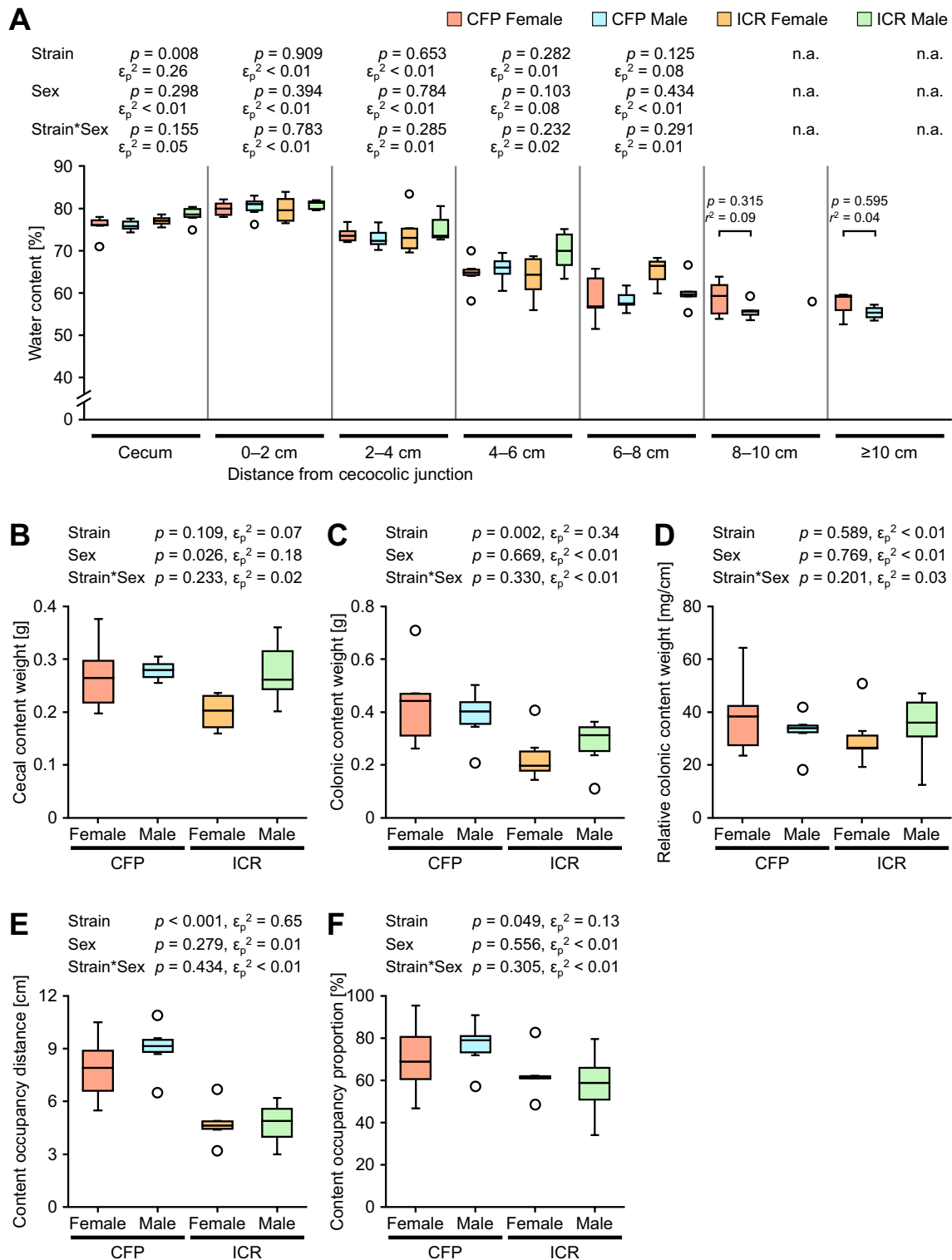
The segment-specific transit was also analyzed using a mathematical model. Similar to the gastric emptying rate, the gastric retention time was longer in CFP mice than in ICR mice ($p < 0.001$, $\epsilon_p^2 = 0.41$; Fig. 4A). However, unlike the SI geometric center, no significant difference was found between CFP and ICR mice for SI transit time ($p = 0.150$, $\epsilon_p^2 = 0.05$; Fig. 4B) or SI transit rate ($p = 0.131$, $\epsilon_p^2 = 0.06$; Fig. 4C).

Cecal Retention Time and Colonic Transit Time

In the same mathematical model analysis, the cecal retention and colonic transit times were longer in CFP mice than in ICR mice ($p = 0.016$, $\epsilon_p^2 = 0.22$ for cecum, $p < 0.001$, $\epsilon_p^2 = 0.66$ for colon; Fig. 4D and E). In particular, the median colonic transit time in CFP mice was > 3-fold longer than that in ICR mice, and this difference was pronounced in the proximal colon (Fig. 4G). Additionally, the median colonic transit rate for CFP mice was > 2-fold slower than that for ICR mice ($p = 0.006$, $\epsilon_p^2 = 0.30$; Fig. 4F).

Feeding and Fecal Excretion

We examined whether differences in GITT between CFP and ICR mice were accompanied by differences in feed intake. The feed intake at the age of 10–11 weeks was lower in



CFP mice than in ICR mice ($p = 0.001$, $\epsilon_p^2 = 0.72$; Fig. 5A), which was supported by the difference observed in water intake ($p = 0.007$, $\epsilon_p^2 = 0.55$; Fig. 5B). The dry weight and pellet number of feces per day were lower in CFP mice than

in ICR mice ($p = 0.001$, $\epsilon_p^2 = 0.72$ for dry weight, $p < 0.001$, $\epsilon_p^2 = 0.73$ for pellet number; Fig. 5C and D).

Fig. 7 Comparison of cecal and colonic water contents and amounts between CFP and ICR mice. At the age of 12 weeks, the following were measured: cecal and colonic water contents (A); cecal content weight (B); colonic content weight (C) and relative weight (D); and content occupancy distance (E) and proportion (F) in the colon. $n=6$ per group, except for colonic water content measurement in 10 cm \leq ($n=3$) in female CFP mice; 8–10 cm ($n=5$) and 10 cm \leq ($n=4$) in male CFP mice; 4–6 cm ($n=5$), 6–8 cm ($n=3$), 8–10 cm ($n=0$), and 10 cm \leq ($n=0$) in female ICR mice; and 0–2 cm ($n=5$), 2–4 cm ($n=5$), 6–8 cm ($n=5$), 8–10 cm ($n=1$), and 10 cm \leq ($n=0$) in male ICR mice. The box plot shows the median and IQR with whiskers extending to the minimum and maximum values within 1.5 times of the IQR from the hinge of the box; data points outside 1.5 times the IQR are shown as circles. Effects of mouse strain (CFP vs. ICR) and sex (female vs. male) and their interaction (Strain*Sex) were analyzed using ART two-way ANOVA or Mann–Whitney U test; p values and effect sizes (ϵ_p^2 , r^2) are shown. See Online Resource 3 for results of post hoc analyses. IQR interquartile range, ART aligned rank transform, ANOVA analysis of variance

Fecal Water Content

To examine the impact of prolonged transit time on water absorption in the colon, fecal water content was determined. As shown in Fig. 6, fecal water content was lower in CFP mice than in ICR mice ($p < 0.001$, $\epsilon_p^2 = 0.49$); however, no significant differences were observed between females and males ($p = 0.614$, $\epsilon_p^2 < 0.01$).

Cecal and Colonic Water Contents

Because the lower fecal water content in CFP mice may have been influenced by the lower colonic transit rate or the longer colon, the cecal and colonic water contents were determined. The cecal water content was lower in CFP mice than in ICR mice ($p = 0.008$, $\epsilon_p^2 = 0.26$; Fig. 7A); however, no significant differences in the colonic water content were observed between the strains at the same distance from the cecocolic junction ($p \geq 0.125$, $\epsilon_p^2 \leq 0.08$).

Amount of Cecal and Colonic Contents

The amounts of cecal and colonic contents were measured to determine whether they were affected by the low feed intake in CFP mice. No significant difference in cecal content weight was observed between CFP and ICR mice ($p = 0.109$, $\epsilon_p^2 = 0.07$; Fig. 7B), and the cecal content weight was lower in females than in males ($p = 0.026$, $\epsilon_p^2 = 0.18$). The colonic content weight was greater in CFP mice than in ICR mice ($p = 0.002$, $\epsilon_p^2 = 0.34$; Fig. 7C); however, no significant differences were observed in the weight of contents per length of the colon between the strains ($p = 0.589$, $\epsilon_p^2 < 0.01$; Fig. 7D). Conversely, the distance occupied by the contents in the colon was greater

in CFP mice ($p < 0.001$, $\epsilon_p^2 = 0.65$; Fig. 7E), even when corrected for colon length ($p = 0.049$, $\epsilon_p^2 = 0.13$; Fig. 7F).

Histological Analysis of Colon

We investigated whether differences in colonic transit between CFP and ICR mice were accompanied by histopathological changes. No histopathological alterations, including tumor and inflammation, were observed across the entire colon of males of either strain. The thickness of the colonic muscle layer did not differ significantly between the strains ($p = 0.784$, $r^2 = 0.02$; Online Resource 2).

Cecal and Fecal Microbiota

Similarity Between Cecal and Fecal Microbiota of CFP and ICR Mice

Cecal and fecal microbiota of CFP and ICR mice were compared using PCoA on the unweighted and weighted UniFrac distances (Fig. 8A and B). These analyses showed that cecal and fecal microbiota were clearly distinct between mouse strains ($p = 0.001$, $r^2 = 0.45$ – 0.70). In CFP mice, cecal and fecal microbiota were significantly different in terms of comparisons based on unweighted and weighted UniFrac distances ($p = 0.001$, $r^2 = 0.13$ for unweighted UniFrac distance; $p = 0.001$, $r^2 = 0.62$ for weighted UniFrac distance). Conversely, in ICR mice, a comparison based on the unweighted UniFrac distance showed no significant difference between cecal and fecal microbiota ($p = 0.913$, $r^2 = 0.02$), but a weighted UniFrac distance showed a significant difference ($p = 0.022$, $r^2 = 0.13$). Additionally, unweighted and weighted UniFrac distances between cecal and fecal microbiota were greater in CFP mice than in ICR mice (Fig. 8C and D).

Alpha Diversity of Cecal and Fecal Microbiota of CFP and ICR Mice

Alpha diversities as assessed based on observed features, Shannon index, and Faith's PD were lower in CFP mice than in ICR mice (Fig. 8E–G). In CFP mice, the observed features and Shannon index were higher in cecal contents than in feces ($p = 0.017$, $r^2 = 0.37$ for observed features; $p = 0.013$, $r^2 = 0.28$ for Shannon index), but no significant differences were observed in ICR mice ($p = 1.000$, $r^2 \leq 0.06$). For Faith's PD, no significant difference was observed between cecal and fecal contents ($p = 0.062$, $\epsilon_p^2 = 0.11$).

Relative Abundance at the Phylum Level

As indicated in Fig. 9A and Table 1, the cecal and fecal microbiota in CFP and ICR mice were dominated by

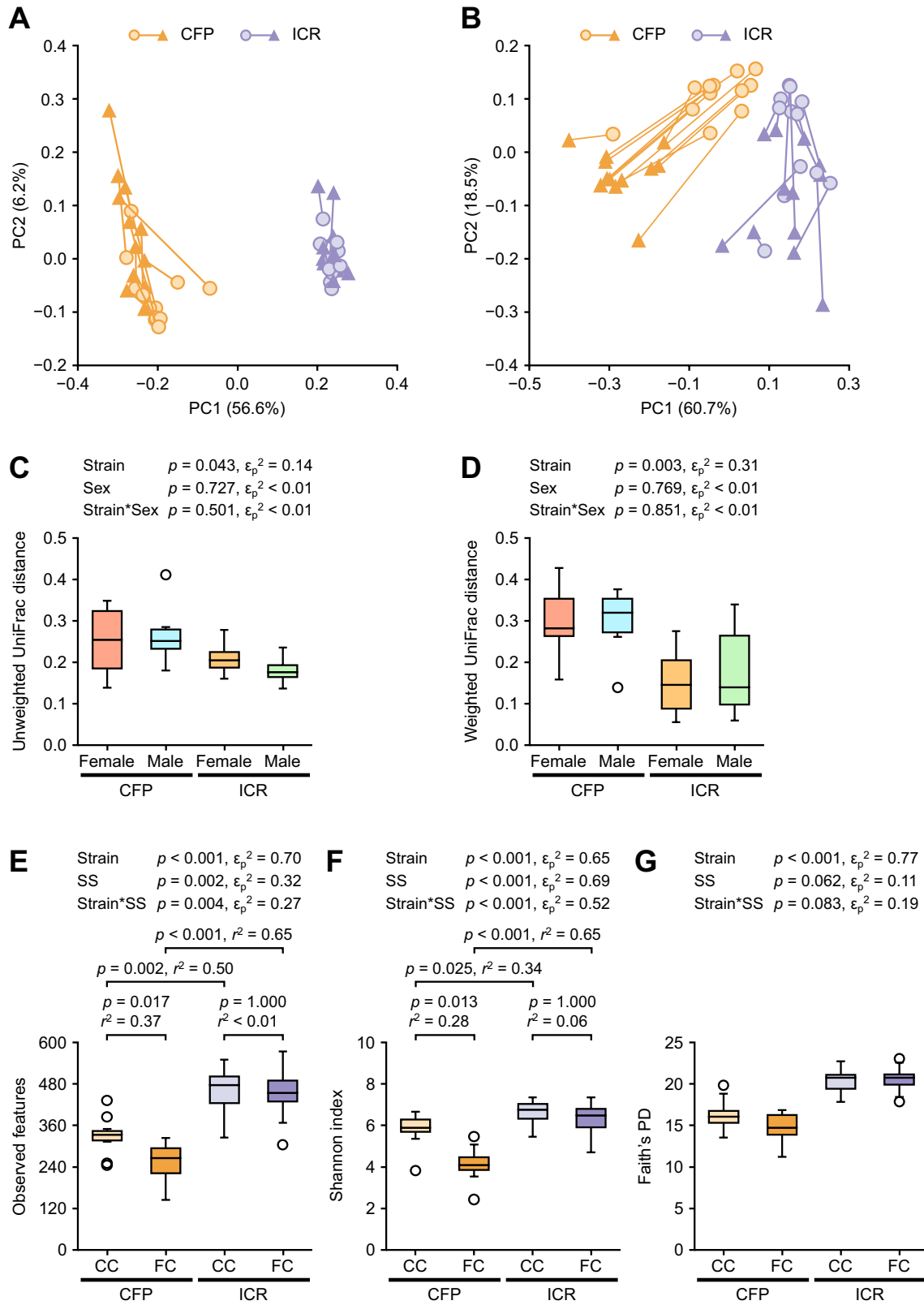


Fig. 8 Analysis of beta and alpha diversities of gut microbiota in CFP and ICR mice. Differences in microbiota between samples were assessed based on unweighted (A) and weighted (B) UniFrac distances and visualized using principal coordinate analysis (circles, cecal contents; triangles, fecal contents; $n=12$ per mouse strain). Unweighted (C) and weighted (D) UniFrac distances between cecal and fecal microbiota were calculated for each group ($n=6$ per group). For alpha diversity, observed features (E), Shannon index (F), and Faith's PD (G) were calculated ($n=12$ per mouse strain). The box plot shows the median and IQR with whiskers extending to the minimum and maximum values within 1.5 times of the IQR from the hinge of the box; data points outside 1.5 times the IQR are shown as circles. Effects of mouse strain (CFP vs. ICR) and sex (female vs. male) and their interactions (Strain*Sex) were analyzed using ART two-way ANOVA; effects of mouse strain, SS (cecal contents vs. fecal contents), and their interactions (Strain*SS) were analyzed using ART two-way repeated measures ANOVA; p values and effect sizes (ϵ_p^2) are shown at the top. In case of significant interactions, p values and effect sizes (r^2) of post hoc Mann–Whitney U test and Wilcoxon signed-rank test with Bonferroni correction are shown immediately above the plot. See Online Resource 3 for results of other post hoc analyses. SS sampling source, CC cecal content, FC fecal content, Faith's PD Faith's phylogenetic diversity, IQR interquartile range, ART aligned rank transform, ANOVA analysis of variance

Firmicutes, followed by Bacteroidota, and these two phyla constituted >95% of the total bacteria detected. For the relative abundance of these two phyla, the interaction between mouse strain and sampling sources were significant ($p=0.040$, $\epsilon_p^2=0.14$ for Firmicutes; $p=0.024$, $\epsilon_p^2=0.17$ for Bacteroidota). Compared to ICR mice, CFP mice had a higher relative abundance of Firmicutes and a lower relative abundance of Bacteroidota in cecal and fecal microbiota. Furthermore, ICR mice exhibited increased abundance of Bacteroidota and decreased abundance of Firmicutes in feces compared to cecal contents, whereas CFP mice exhibited no significant difference in the abundance of either

phylum between cecal and fecal contents. The ratio of Firmicutes to Bacteroidota (F/B ratio) was lower in fecal contents compared to cecal contents ($p=0.001$, $\epsilon_p^2=0.35$) and was higher in CFP mice than in ICR mice ($p<0.001$, $\epsilon_p^2=0.50$).

Relative Abundance at the Family Level

Figure 9B shows the relative abundance of bacteria at the family level, and Table 2 shows the top three families in either the cecal or fecal contents of CFP or ICR mice. For Erysipelotrichaceae and Lachnospiraceae, both members of the phylum Firmicutes, the interaction between mouse strain and sampling source was significant ($p<0.001$, $\epsilon_p^2=0.82$ for Erysipelotrichaceae; $p<0.001$, $\epsilon_p^2=0.42$ for Lachnospiraceae). The abundance of Erysipelotrichaceae was higher in CFP mice than in ICR mice ($p<0.001$; $\epsilon_p^2=0.83$) and was higher in fecal contents than in cecal contents in CFP mice; however, no significant difference was observed in ICR mice. The abundance of Lachnospiraceae decreased in fecal contents compared to cecal contents in both CFP and ICR mice, with a more pronounced decrease in CFP mice. Muribaculaceae, belonging to the phylum Bacteroidota, was less abundant in CFP mice than in ICR mice ($p<0.001$, $\epsilon_p^2=0.64$).

Discussion

This study revealed that CFP mice exhibited a longer GITT compared to ICR mice. GITT can be influenced by many factors [1, 2]. Among these, this study evaluated the effects of strain, specifically genetic factors and sex on GITT. The GI length, which is generally positively correlated with body weight [28], is another factor that may influence GITT. CFP

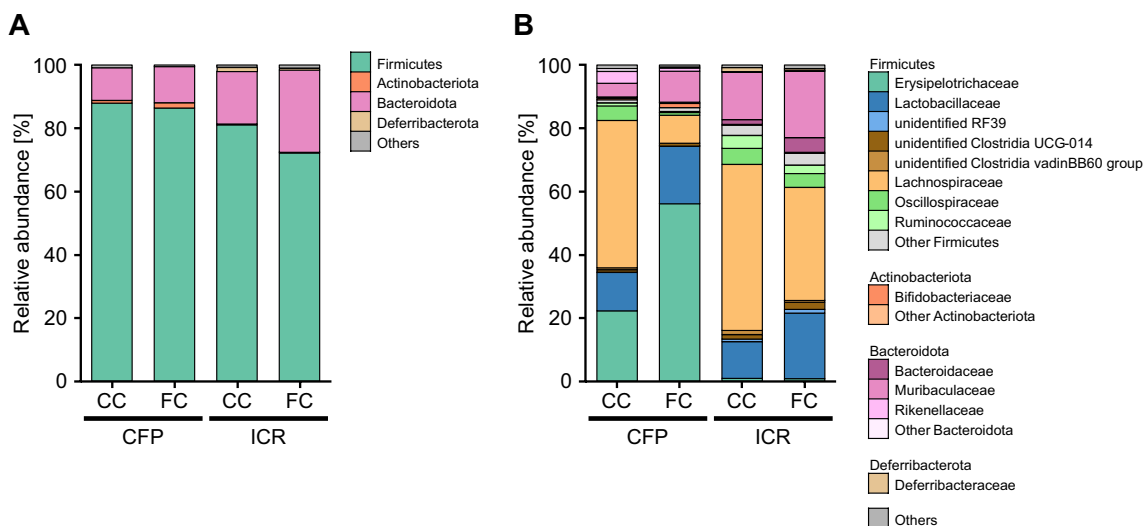


Fig. 9 Relative abundance of bacterial groups in CC and FC of CFP and ICR mice at the phylum (A) and family (B) level. $n=12$ per mouse strain. CC cecal content, FC fecal content

Table 1 Comparison of the relative abundances of Firmicutes and Bacteroidota and their ratios between CFP and ICR mice and between their cecal and fecal contents

	CFP mice		ICR mice		<i>p</i> value		
	Cecal content	Fecal content	Cecal content	Fecal content	Strain	SS	Strain*SS
Firmicutes [%]	89.6 [88.4, 90.9] ^b	86.5 [85.6, 87.6] ^c	83.4 [75.0, 87.4] ^{a,b}	74.8 [70.2, 77.6] ^{a,c}	<0.001	0.001	0.040
Bacteroidota [%]	8.5 [7.7, 9.6] ^b	11.6 [10.4, 12.5] ^c	14.4 [9.9, 22.5] ^{a,b}	23.0 [20.5, 28.5] ^{a,c}	<0.001	<0.001	0.024
F/B ratio	10.5 [9.3, 11.9]	7.5 [6.9, 8.5]	5.8 [3.4, 8.8]	3.3 [2.5, 3.8]	<0.001	0.001	0.725

Data are presented as medians [interquartile ranges]. There were six female and six male mice per strain. The *p* values of aligned rank transform two-way repeated measures analysis of variance are shown on the right (Strain, effect of strain; SS, effect of SS; Strain*SS, interaction of strain and SS; bold: *p* < 0.05). Values with the same letter are significantly different (*p* < 0.05) according to post hoc Wilcoxon signed-rank test and Mann–Whitney *U* test with Bonferroni correction when the interaction of strain and SS is significant. See Online Resource 3 for results of other post hoc analyses. SS sampling source (cecal and fecal contents), F/B ratio of Firmicutes to Bacteroidota

mice weigh more than commonly used inbred strains, such as C57BL/6 and BALB/c mice; therefore, they may have a longer GI tract than these commonly used strains. Hence, we used ICR mice, a large and widely used outbred strain, as the control strain, allowing comparisons with random genetic populations rather than specific genetic backgrounds. Although CFP mice weighed more than ICR mice, they exhibited a shorter small intestine. Conversely, the median colonic length was 1.4-fold longer in CFP mice than in ICR mice. This difference in colonic length cannot be explained by differences in body weight. These differences in the GI length should be considered in comparing the GITTs of the two strains.

GIT was evaluated using well-established indices, including WGTT, MRT, gastric emptying rate, and SI geometric center [29], and a mathematical model. WGTT and MRT serve as indices for the total GI tract transit. WGTT reflects only the time required for the fastest transit of contents through the entire GI tract, whereas MRT also reflects retention in the stomach and cecum as well as reverse peristalsis in the small intestine and colon. Both WGTT and MRT indicated that CFP mice exhibited slower transit throughout the GI tract compared to ICR mice. WGTT has been reported to range 2–6 h for widely used inbred mouse strains, such

as C57BL/6 and BALB/c [30–32]. In another inbred mouse strain, C3H, orally administered markers reached the distal colon within 3 h [33]. MRT has been reported to be approximately 10.3 h in DBA/2 J mice [34]. Consequently, CFP mice are likely to exhibit slower transit throughout the GI tract than commonly used inbred mouse strains.

The transit through anatomical segments within the GI tract was examined to better understand the differences in GIT between CFP and ICR mice. Gastric emptying rate and retention time, representing the fraction of volume leaving the stomach in a given time and the time for a specified fraction of contents to exit the stomach, respectively, serve as indices of gastric transit. Both indices revealed that CFP mice exhibited slower gastric transit compared to ICR mice. The SI geometric center showed slower SI transit in CFP mice, whereas no significant differences were observed in SI transit time or rate between the two strains. This inconsistency may indicate that the fastest transit in the small intestine is similar in both strains, but factors such as content agitation or reverse peristalsis have a more pronounced impact on SI transit in CFP mice. Alternatively, transit in the upper small intestine might be slower in CFP mice than in ICR mice, yet consistent throughout the small intestine, as reflected by the SI geometric center measured shortly

Table 2 Comparison of the relative abundances of bacterial taxa at the family level between CFP and ICR mice and between their cecal and fecal contents

	CFP mice		ICR mice		<i>p</i> value		
	Cecal content	Fecal content	Cecal content	Fecal content	Strain	SS	Strain*SS
Erysipelotrichaceae [%]	24.2 [12.6, 28.1] ^{a,b}	59.9 [43.7, 63.6] ^{a,c}	0.9 [0.7, 1.0] ^b	0.8 [0.6, 0.9] ^c	<0.001	<0.001	<0.001
Lactobacillaceae [%]	8.5 [6.9, 12.8]	16.2 [12.0, 22.6]	8.9 [6.3, 14.5]	20.2 [7.6, 23.6]	0.792	0.001	0.562
Lachnospiraceae [%]	47.5 [43.0, 54.2] ^a	5.8 [3.3, 11.0] ^{a,c}	53.9 [48.3, 59.3] ^b	39.4 [24.6, 47.6] ^{b,c}	<0.001	<0.001	<0.001
Muribaculaceae [%]	3.8 [3.2, 4.5]	9.9 [8.4, 10.6]	11.9 [8.9, 20.8]	18.4 [14.4, 25.7]	<0.001	<0.001	0.951

Data are presented as medians [interquartile ranges]. There were six female and six male mice per strain. The *p* value of aligned rank transform two-way repeated measures analysis of variance are shown on the right (Strain, effect of strain; SS, effect of SS; Strain*SS, interaction of strain and SS; bold: *p* < 0.05). Values with the same letter are significantly different (*p* < 0.05) according to post hoc Wilcoxon signed-rank test and Mann–Whitney *U* test with Bonferroni correction when the interaction of strain and SS is significant. See Online Resource 3 for results of other post hoc analyses. SS sampling source (cecal and fecal contents)

after marker administration. Further clarification could be achieved through mathematical modeling, particularly with a segmented small intestine. In the large intestine, which constitutes the majority of the total GIT [17], cecal retention time and colonic transit time were longer in CFP mice than in ICR mice. The colonic transit rate was also lower in CFP mice than in ICR mice, indicating slower colonic transit even when accounting for differences in colonic length. These findings suggest that CFP mice have an overall slower GIT due to delayed transit in each segment of the GI tract, although the specific contribution of the small intestine remains unclear.

CFP mice exhibited a lower daily fecal output compared to ICR mice, likely attributed to their reduced feed intake. Interestingly, despite the lower feed intake, the amount of colonic content was greater in CFP mice, suggesting that delayed colonic transit led to content retention in the colon, similar to constipation. This content retention in the colon may enhance colonic water absorption, resulting in decreased fecal water content. The fecal water content was lower in CFP mice than in ICR mice, whereas no significant difference in colonic water content was observed between these strains at the same distance from the cecocolic junction. These results indicate that the lower fecal water content in CFP mice does not result from increased water absorption during their slow transit through the colon but rather from the extended length of their colon.

The analyses of unweighted and weighted UniFrac distances revealed greater differences between cecal and fecal microbiota in CFP mice than in ICR mice. This could be because the microbiota undergoes more significant changes during colonic transit, which is longer in CFP mice. Another explanation could be that the difference reflects diurnal variation in gut microbiota [35], as contents leaving the cecum at earlier time points may be excreted as feces in CFP mice. Therefore, to clarify the cause of the difference between cecal and fecal microbiota, microbiota from samples collected at multiple time points should be analyzed.

Delayed GIT could be caused by organic or functional disorders [36]. No organic disorders, including tumors or inflammation, were observed in the colon of CFP mice, and no physical obstruction to the passage of contents was suspected. Other organic or functional disorders in CFP mice were not evident in this study. Nevertheless, the phenotype of CFP mice exhibited some similarities to constipation mouse models and patients with constipation.

Delayed colonic transit, along with delayed transit of the entire GI tract and stomach, has been observed in patients with constipation [37]. The low fecal weights and pellet numbers are consistent with findings from previously reported constipation mouse models [12, 13, 38, 39], and some of these models showed low feed intakes [38, 39]. Conversely, no significant difference was found between

male CFP and ICR mice in the thickness of the colonic muscle layer, which is often thinner in constipation mouse models [12, 13, 39–41].

Changes in gut microbiota composition are also observed in constipated mice and humans. Similar to CFP mice, higher abundance of Firmicutes and lower abundance of Bacteroidota or a higher F/B ratio have been reported in constipation mouse models, mice with delayed GIT [5, 42, 43], and patients with constipation [44–46]; however, opposite findings have also been reported in constipated mice [13, 38, 40, 41, 47, 48] and humans [49, 50]. Gut microbiota composition is influenced by the gut environment, and different types of constipation may lead to different gut environments, resulting in distinct gut microbiota compositions [51]. The association between delayed colonic transit and gut microbiota in CFP mice with respect to genetic influence was considered as follows. Host genetic differences may influence both colonic transit [52] and gut microbiota composition [53, 54]. Host genetic factors affecting the gut microbiota are not fully understood but may include differences in immunoglobulins secreted into the intestinal lumen and bile acid metabolism [54]. Additionally, as evidenced by the delayed GIT in mice transplanted with cecal microbiota from loperamide-induced constipated mice [38], gut microbiota may delay GIT. Therefore, the association between differences in GIT and gut microbiota between CFP and ICR mice could involve (1) the differences in GIT caused by host genetic differences resulting in differences in the gut microbiota and (2) host genetic differences affecting the gut microbiota through factors other than GIT, and the gut microbiota affecting the GIT or both (1) and (2). Given the similarity of the gut microbiota of CFP mice to that of other constipated mice, as described above, it is reasonable to assume that the gut microbiota of CFP mice is correlated with delayed GIT. Thus, delayed colonic transit in CFP mice may be associated with functional changes involving the gut microbiota.

A large amount of content was present in the colon of CFP mice. In mice, the presence of a large amount of content in the colon has been reported to cause colonic elongation and decrease the frequency of the colonic migrating motor complex, which drives colonic content propulsion [55]. In humans, the relationship between colonic transit and colonic length is not well understood [56]; however, an association between low defecation frequency and prolonged colon or colonic transit time has recently been reported [57, 58]. If the long colon of CFP mice is indeed due to elongation, they may represent the first spontaneous model of delayed colonic transit with colonic elongation.

This study demonstrated that CFP mice had a longer GIT due to a longer colon and a slower colonic transit rate compared to ICR mice. Although host genetic factors, gut microbiota, or a combination of both may contribute to the GIT characteristics of CFP mice, the underlying mechanism

remains unclear. To elucidate this mechanism, neurochemical, functional, and pharmacological analyses are necessary. Investigations on methods for controlling the gut microbiota and analyses of gut bacterial metabolites would also be valuable. Additionally, the effect of sex on the GITT of CFP mice is challenging to conclusively determine from this study. In humans, women have been reported to have longer colons [58] and longer transit times throughout the GI tract and colon [59] than men. However, the effects of sex on GI length and transit time have rarely been reported in mice. Therefore, it is unclear whether species differences or other factors account for the lack of significant sex differences observed in this study.

In conclusion, CFP mice, characterized by a longer colon, exhibit slow retention and transit of fluid in every segment of their GI tract, except the small intestine. These traits in CFP mice may influence their cecal and fecal microbiota, contributing to a better understanding of GI physiology and disease.

Supplementary Information The online version contains supplementary material available at <https://doi.org/10.1007/s10620-024-08420-x>.

Acknowledgments We thank Tomonori Aida for providing excellent technical assistance and our colleagues for maintaining CFP/Yit mice.

Author's contribution GW, TS, and KK conceived the study. GW, MT, HN, JO, YO, TS, and KK designed the study. AK, TS, and KK supervised the study. GW, MT, HN, JO, TS, and KK acquired the data. GW, MT, TK, HN, TS, and KK analyzed the data. GW and KK drafted the manuscript. All authors interpreted the data, revised the manuscript critically, and approved the final version of the article.

Funding This study was conducted with funding from Yakult Honsha Co., Ltd.

Declarations

Conflict of interest All authors are employees of Yakult Honsha Co., Ltd.

Ethical approval All procedures involving animals were conducted in compliance with the Japanese Law for the Humane Treatment and Management of Animals (Law No. 105, issued on October 1, 1973). All animal experiments were reviewed by the Institutional Animal Care and Use Committee of Yakult Central Institute and approved by the Director of the Yakult Central Institute (Approval Numbers: 21-017, 21-040, 21-050, 21-099, and 22-034). All animals were cared for and used under a program accredited by AAALAC International.

Open Access This article is licensed under a Creative Commons Attribution-NonCommercial 4.0 International License, which permits any non-commercial use, sharing, adaptation, distribution and reproduction in any medium or format, as long as you give appropriate credit to the original author(s) and the source, provide a link to the Creative Commons licence, and indicate if changes were made. The images or other third party material in this article are included in the article's Creative Commons licence, unless indicated otherwise in a credit line to the material. If material is not included in the article's Creative Commons licence and your intended use is not permitted by statutory

regulation or exceeds the permitted use, you will need to obtain permission directly from the copyright holder. To view a copy of this licence, visit <http://creativecommons.org/licenses/by-nc/4.0/>.

References

1. Procházková N, Falony G, Dragsted LO et al. Advancing human gut microbiota research by considering gut transit time. *Gut*. 2023;72:180–191.
2. Waclawiková B, Codutti A, Alim K, El Aidy S. Gut microbiota-motility interregulation: insights from *in vivo*, *ex vivo* and *in silico* studies. *Gut Microbes*. 2022;14:1997296.
3. Kashyap PC, Marcobal A, Ursell LK et al. Complex interactions among diet, gastrointestinal transit, and gut microbiota in humanized mice. *Gastroenterology*. 2013;144:967–977.
4. Kongdang P, Pruksakorn D, Koonrunsesomboon N. Preclinical experimental models for assessing laxative activities of substances/products under investigation: a scoping review of the literature. *Am J Transl Res*. 2022;14:698–717.
5. Lin X, Liu Y, Ma L et al. Constipation induced gut microbiota dysbiosis exacerbates experimental autoimmune encephalomyelitis in C57BL/6 mice. *J Transl Med*. 2021;19:317.
6. Mukai R, Handa O, Naito Y et al. High-fat diet causes constipation in mice via decreasing colonic mucus. *Dig Dis Sci*. 2020;65:2246–2253.
7. Kakino M, Tazawa S, Maruyama H et al. Laxative effects of agarwood on low-fiber diet-induced constipation in rats. *BMC Complement Altern Med*. 2010;10:68.
8. Ge X, Zhao W, Ding C et al. Potential role of fecal microbiota from patients with slow transit constipation in the regulation of gastrointestinal motility. *Sci Rep*. 2017;7:441.
9. Liang C, Wang KY, Yu Z, Xu B. Development of a novel mouse constipation model. *World J Gastroenterol*. 2016;22:2799–2810.
10. Anderson G, Noorian AR, Taylor G et al. Loss of enteric dopaminergic neurons and associated changes in colon motility in an MPTP mouse model of Parkinson's disease. *Exp Neurol*. 2007;207:4–12.
11. Li Z, Chalazonitis A, Huang YY et al. Essential roles of enteric neuronal serotonin in gastrointestinal motility and the development/survival of enteric dopaminergic neurons. *J Neurosci*. 2011;31:8998–9009.
12. Kim JE, Choi YJ, Lee SJ et al. Molecular characterization of constipation disease as novel phenotypes in CRISPR-Cas9-Generated leptin knockout mice with obesity. *Int J Mol Sci*. 2020;21:9464.
13. Choi YJ, Kim JE, Lee SJ et al. Dysbiosis of fecal microbiota from complement 3 knockout mice with constipation phenotypes contributes to development of defecation delay. *Front Physiol*. 2021;12:650789.
14. Mulè F, Amato A, Serio R. Gastric emptying, small intestinal transit and fecal output in dystrophic (mdx) mice. *J Physiol Sci*. 2010;60:75–79.
15. Kishi K, Kamizaki M, Kaji N, Iino S, Hori M. A close relationship between networks of interstitial cells of Cajal and gastrointestinal transit *in vivo*. *Front Pharmacol*. 2020;11:587453.
16. Funabashi H, Okabe Y, Shinpo A, inventors; Yakult Honsha Co., Ltd., assignee. [Mice with abnormal gastrointestinal tract function and use of them]. Japanese patent JP 3957489. August 15, 2007. Japanese.

17. Hendriks WH, van Baal J, Bosch G. Ileal and faecal protein digestibility measurement in humans and other non-ruminants - a comparative species view. *Br J Nutr.* 2012;108:S247–S257.
18. Degen LP, Phillips SF. How well does stool form reflect colonic transit? *Gut.* 1996;39:109–113.
19. Koopman JP, Kennis HM, van Druten JAM. Colonization resistance of the digestive tract and gastro-intestinal transit time in SPF mice. *Lab Anim.* 1978;12:223–226.
20. Blaxter KL, Graham NM, Wainman FW. Some observations on the digestibility of food by sheep, and on related problems. *Br J Nutr.* 1956;10:69–91.
21. Mathers JC, Smith H, Carter S. Dose-response effects of raw potato starch on small-intestinal escape, large-bowel fermentation and gut transit time in the rat. *Br J Nutr.* 1997;78:1015–1029.
22. Miller MS, Galligan JJ, Burks TF. Accurate measurement of intestinal transit in the rat. *J Pharmacol Methods.* 1981;6:211–217.
23. Schneider CA, Rasband WS, Eliceiri KW. NIH Image to ImageJ: 25 years of image analysis. *Nat Methods.* 2012;9:671–675.
24. Caporaso JG, Lauber CL, Walters WA et al. Ultra-high-throughput microbial community analysis on the Illumina HiSeq and MiSeq platforms. *ISME J.* 2012;6:1621–1624.
25. Togao M, Kurakawa T, Tajima S et al. Human gut microbiota influences drug-metabolizing enzyme hepatic Cyp3a: A human flora-associated mice study. *J Toxicol Sci.* 2023;48:333–343.
26. Bolyen E, Rideout JR, Dillon MR et al. Reproducible, interactive, scalable and extensible microbiome data science using QIIME 2. *Nat Biotechnol.* 2019;37:852–857.
27. Wobbrock JO, Findlater L, Gergle D, et al. The aligned rank transform for nonparametric factorial analyses using only ANOVA procedures. In: Proceedings of the SIGCHI Conference on Human Factors in Computing Systems. New York, NY: Association for Computing Machinery; 2011:143–146.
28. Ogiolda L, Wanke R, Rottmann O, Hermanns W, Wolf E. Intestinal dimensions of mice divergently selected for body weight. *Anat Rec.* 1998;250:292–299.
29. Camilleri M, Linden DR. Measurement of gastrointestinal and colonic motor functions in humans and animals. *Cell Mol Gastroenterol Hepatol.* 2016;2:412–428.
30. Margolis KG, Stevanovic K, Li Z et al. Pharmacological reduction of mucosal but not neuronal serotonin opposes inflammation in mouse intestine. *Gut.* 2014;63:928–937.
31. Chandrasekharan B, Saeedi BJ, Alam A et al. Interactions between commensal bacteria and enteric neurons, via FPR1 induction of ROS, increase gastrointestinal motility in mice. *Gastroenterology.* 2019;157:179–192.e2.
32. Gama LA, Rocha Machado MP, Beckmann APS, Miranda JRA, Corá LA, Américo MF. Gastrointestinal motility and morphology in mice: strain-dependent differences. *Neurogastroenterol Motil.* 2020;32:e13824.
33. Woting A, Blaut M. Small intestinal permeability and gut-transit time determined with low and high molecular weight fluorescein isothiocyanate-dextran in C3H mice. *Nutrients.* 2018;10:685.
34. Bellier S, Da Silva NR, Aubin-Houzelstein G, Elbaz C, Vanderwinden JM, Panthier JJ. Accelerated intestinal transit in inbred mice with an increased number of interstitial cells of Cajal. *Am J Physiol Gastrointest Liver Physiol.* 2005;288:G151–G158.
35. Zarrinpar A, Chaix A, Yooshep S, Panda S. Diet and feeding pattern affect the diurnal dynamics of the gut microbiome. *Cell Metab.* 2014;20:1006–1017.
36. Andrews CN, Storr M. The pathophysiology of chronic constipation. *Can J Gastroenterol.* 2011;25:16B–21B.
37. Rao SS, Kuo B, McCallum RW et al. Investigation of colonic and whole-gut transit with wireless motility capsule and radio-paque markers in constipation. *Clin Gastroenterol Hepatol.* 2009;7:537–544.
38. Touw K, Ringus DL, Hubert N et al. Mutual reinforcement of pathophysiological host–microbe interactions in intestinal stasis models. *Physiol Rep.* 2017;5:e13182.
39. Li C, Li Z, Wu H et al. Therapeutic effect of *Moringa oleifera* leaves on constipation mice based on pharmacodynamics and serum metabolomics. *J Ethnopharmacol.* 2022;282:114644.
40. He Q, Han C, Huang L et al. Astragaloside IV alleviates mouse slow transit constipation by modulating gut microbiota profile and promoting butyric acid generation. *J Cell Mol Med.* 2020;24:9349–9361.
41. Qiu B, Zhu L, Zhang S et al. Prevention of loperamide-induced constipation in mice and alteration of 5-hydroxytryptamine signaling by *Ligilactobacillus salivarius* Li01. *Nutrients.* 2022;14:4083.
42. Anitha M, Reichardt F, Tabatabavakili S et al. Intestinal dysbiosis contributes to the delayed gastrointestinal transit in high-fat diet fed mice. *Cell Mol Gastroenterol Hepatol.* 2016;2:328–339.
43. Yao Z, Fu S, Ren B, Ma L, Sun D. Based on network pharmacology and gut microbiota analysis to investigate the mechanism of the laxative effect of pterostilbene on loperamide-induced slow transit constipation in mice. *Front Pharmacol.* 2022;13:913420.
44. Zhu L, Liu W, Alkhouri R et al. Structural changes in the gut microbiome of constipated patients. *Physiol Genomics.* 2014;46:679–686.
45. Tian H, Chen Q, Yang B, Qin H, Li N. Analysis of gut microbiome and metabolite characteristics in patients with slow transit constipation. *Dig Dis Sci.* 2021;66:3026–3035.
46. Xu Y, Shao M, Fang X et al. Antipsychotic-induced gastrointestinal hypomotility and the alteration in gut microbiota in patients with schizophrenia. *Brain Behav Immun.* 2022;99:119–129.
47. Ren X, Liu L, Gamallat Y, Zhang B, Xin Y. Enteromorpha and polysaccharides from *Enteromorpha* ameliorate loperamide-induced constipation in mice. *Biomed Pharmacother.* 2017;96:1075–1081.
48. Qiao Y, Qiu Z, Tian F et al. *Pediococcus acidilactici* strains improve constipation symptoms and regulate intestinal flora in mice. *Front Cell Infect Microbiol.* 2021;11:655258.
49. Vandeputte D, Falony G, Vieira-Silva S, Tito RY, Joossens M, Raes J. Stool consistency is strongly associated with gut microbiota richness and composition, enterotypes and bacterial growth rates. *Gut.* 2016;65:57–62.
50. Tian Y, Zuo L, Guo Q et al. Potential role of fecal microbiota in patients with constipation. *Ther Adv Gastroenterol.* 2020;13:1756284820968423.
51. Yang L, Wang Y, Zhang Y et al. Gut microbiota: a new avenue to reveal pathological mechanisms of constipation. *Appl Microbiol Biotechnol.* 2022;106:6899–6913.
52. Bonfiglio F, Liu X, Smillie C et al. GWAS of stool frequency provides insights into gastrointestinal motility and irritable bowel syndrome. *Cell Genom.* 2021. <https://doi.org/10.1016/j.xgen.2021.100069>.
53. Friswell MK, Gika H, Stratford IJ et al. Site and strain-specific variation in gut microbiota profiles and metabolism in experimental mice. *PLOS ONE.* 2010;5:e8584.
54. Org E, Parks BW, Joo JWJ et al. Genetic and environmental control of host–gut microbiota interactions. *Genome Res.* 2015;25:1558–1569.
55. Heredia DJ, Dickson EJ, Bayguinov PO, Hennig GW, Smith TK. Colonic elongation inhibits pellet propulsion and migrating motor complexes in the murine large bowel. *J Physiol.* 2010;588:2919–2934.
56. Müller-Lissner SA, Kamm MA, Scarpignato C, Wald A. Myths and misconceptions about chronic constipation. *Am J Gastroenterol.* 2005;100:232–242.

57. Raahave D, Christensen E, Loud FB, Knudsen LL. Correlation of bowel symptoms with colonic transit, length, and faecal load in functional faecal retention. *Dan Med Bull.* 2009;56:83–88.
58. Utano K, Nagata K, Honda T, Kato T, Lefor AK, Togashi K. Bowel habits and gender correlate with colon length measured by CT colonography. *Jpn J Radiol.* 2022;40:298–307.
59. Southwell BR, Clarke MCC, Sutcliffe J, Hutson JM. Colonic transit studies: normal values for adults and children with comparison of radiological and scintigraphic methods. *Pediatr Surg Int.* 2009;25:559–572.

Publisher's Note Springer Nature remains neutral with regard to jurisdictional claims in published maps and institutional affiliations.